

Unambiguous exclusion of *d*-wave gap symmetry in high-temperature superconductors

Guo-meng Zhao*

Department of Physics and Astronomy, California State University at Los Angeles, Los Angeles, CA 90032, USA

We report the spectra of the second derivative $-\frac{d^2(\text{Re}\Sigma)}{d\omega^2}$ of the real part of electron self-energy Σ along the diagonal direction (where ω is energy measured from the superconducting gap Δ_D) for a nonsuperconducting $\text{La}_{1.97}\text{Sr}_{0.03}\text{CuO}_4$ crystal and a superconducting $\text{Bi}_2\text{Sr}_2\text{CaCu}_2\text{O}_{8+y}$ crystal with $T_c = 91$ K. For $\text{La}_{1.97}\text{Sr}_{0.03}\text{CuO}_4$ with $\Delta_D = 0$, the energies of the peaks in $-\frac{d^2(\text{Re}\Sigma)}{d\omega^2}$ match precisely with the phonon energies. For $\text{Bi}_2\text{Sr}_2\text{CaCu}_2\text{O}_{8+y}$, the peak energies in $-\frac{d^2(\text{Re}\Sigma)}{d\omega^2}$ also match precisely with the phonon energies obtained from inelastic neutron scattering and single-particle tunneling when Δ_D is set to 7.0 meV. The present results unambiguously demonstrate that the superconducting energy gap along the diagonal direction of $\text{Bi}_2\text{Sr}_2\text{CaCu}_2\text{O}_{8+y}$ is at least 7 meV and that the gap symmetry is not *d*-wave.

The phenomenon of superconductivity involves the pairing of electrons into Cooper pairs [1]. The internal wavefunction (gap function) of these Cooper pairs obeys a certain symmetry which reflects the underlying pairing mechanism. The symmetry of the gap function in high-temperature cuprate superconductors has been a topic of intense debate for over fifteen years. A majority of experiments testing the symmetry (e.g., penetration depth, thermal conductivity, and specific heat measurements) have pointed to the existence of line nodes in the gap function [2–5]. Qualitatively, these experiments are consistent with a *d*-wave gap function with four line nodes. Nevertheless, these data are also consistent with an extended *s*-wave gap function (*s* + *g* wave), which has eight line nodes when the *g*-wave component is larger than the *s*-wave component. Therefore, either *d*-wave or extended *s*-wave gap symmetry is supported by these bulk-sensitive experiments.

There has been much experimental evidence for a *d*-wave symmetry of superconducting condensate (order parameter) for hole-doped cuprate superconductors. In particular, phase-sensitive experiments based on planar Josephson tunneling [6] appear to provide compelling evidence for a *d*-wave order parameter (OP) symmetry. However, since the OP symmetry is not necessarily the same as the gap symmetry [7], these phase-sensitive experiments which are probing the OP symmetry on the underdoped surface region [8,9] do not provide a constraint on the gap symmetry in the bulk. The evidence for a *d*-wave OP symmetry on underdoped surfaces is consistent with a *d*-wave symmetry of the Bose-Einstein condensate of intersite oxygen-hole bipolarons [7], which are the main charge carriers in underdoped cuprates [10].

Because the existence of line nodes in the bulk superconducting gap is consistent either with *d*-wave or extended *s*-wave, a clear distinction between the two contenders can be made if one can precisely determine the superconducting gap along the diagonal direction (45° from the Cu-O bonding direction). Some earlier angle resolved photoemission spectroscopy (ARPES) studies on

$\text{Bi}_2\text{Sr}_2\text{CaCu}_2\text{O}_{8+y}$ (BSCCO) [11–13] led to contradictory conclusions about the magnitude of the gap along the diagonal direction (Δ_D). From the ARPES data obtained with an energy resolution of about 30 meV, Shen *et al.* [11] found $\Delta_D \simeq 0$ for an overdoped BSCCO with $T_c = 78$ K and $\Delta_D \simeq 12$ meV for another BSCCO with $T_c = 86$ K. Ding *et al.* obtained ARPES spectra with a 17 meV energy resolution and showed that $\Delta_D = 3.5 \pm 2.5$ meV (Ref. [12]) or $\Delta_D = 0 \pm 3$ meV (Ref. [13]) in a nearly optimally doped BSCCO (Ref. [12]). On the other hand, with a better energy resolution (about 10 meV) Vobornik *et al.* found $\Delta_D = 9 \pm 2$ meV for a heavily overdoped BSCCO with $T_c = 60$ K (Ref. [14]). Therefore, the evidence for the *d*-wave gap symmetry from these ARPES data is far from conclusive.

On the other hand, there is overwhelming evidence favoring an extended *s*-wave gap [15,16]. This evidence includes data from phase-sensitive experiments based on out-of-plane Josephson tunneling [17–19], single-particle tunneling spectroscopy [20], Raman spectroscopy of heavily overdoped cuprates [21], nonlinear Meissner effect [22], and inelastic neutron scattering [23]. Moreover, the measurements of the physical properties that are related to low energy quasiparticle excitations [2–5] are in quantitative agreement with an extended *s*-wave gap symmetry with eight line nodes [15].

Here, we report the spectra of the second derivative $-\frac{d^2(\text{Re}\Sigma)}{d\omega^2}$ of the real part of electron self-energy Σ along the diagonal direction (where $\omega = E_F - E - \Delta_D$) for a nonsuperconducting $\text{La}_{1.97}\text{Sr}_{0.03}\text{CuO}_4$ (LSCO) crystal and a superconducting $\text{Bi}_2\text{Sr}_2\text{CaCu}_2\text{O}_{8+y}$ crystal with $T_c = 91$ K. For $\text{La}_{1.97}\text{Sr}_{0.03}\text{CuO}_4$ with $\Delta_D = 0$, the energies of the peaks in $-\frac{d^2(\text{Re}\Sigma)}{d\omega^2}$ match precisely with the phonon energies. For $\text{Bi}_2\text{Sr}_2\text{CaCu}_2\text{O}_{8+y}$, the peak energies in $-\frac{d^2(\text{Re}\Sigma)}{d\omega^2}$ also match precisely with the phonon energies obtained from inelastic neutron scattering and single-particle tunneling when Δ_D is set to 7.0 meV. The present results unambiguously demonstrate that the superconducting energy gap along the diagonal direction of $\text{Bi}_2\text{Sr}_2\text{CaCu}_2\text{O}_{8+y}$ is at least 7 meV and

that the gap symmetry is not d -wave.

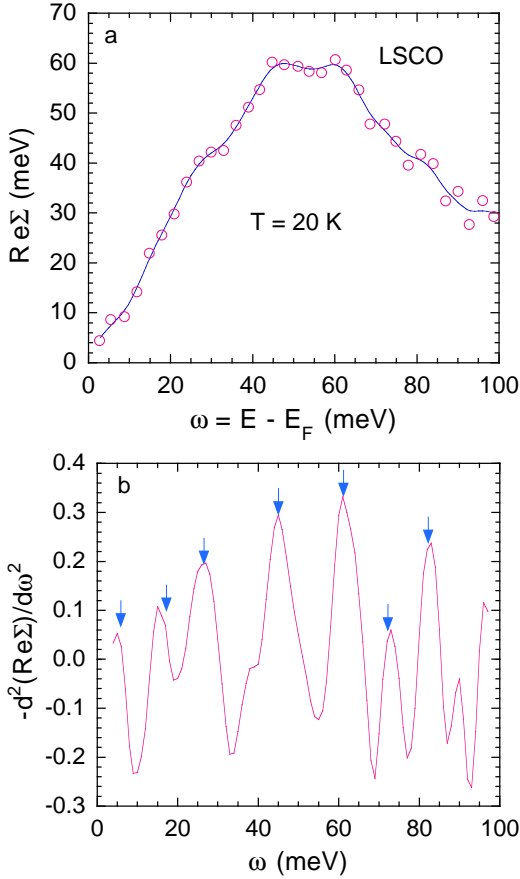


FIG. 1. a) The real part of the electron self-energy at 20 K for a nonsuperconducting $La_{1.97}Sr_{0.03}CuO_4$ crystal. The data are reproduced from Fig. 2 of Ref. [24]. The solid line is a smoothed curve with a smoothing parameter $\Lambda = -2.5$ (see text). b) $-d^2(Re\Sigma)/d\omega^2$ spectrum obtained from the smoothed curve in a). The downward arrows mark the positions of the boson modes in the electron-boson spectral function obtained using a maximum entropy method [24].

In Fig. 1a we plot the real part of the electron self-energy for a nonsuperconducting $La_{1.97}Sr_{0.03}CuO_4$ crystal. The data are reproduced from Fig. 2 of Ref. [24]. The electron self-energy data are obtained from an ARPES spectrum, which is taken with an energy resolution of about 20 meV (Ref. [24]). The Fermi level calibration has a ± 2.5 meV uncertainty [24]. It is apparent that the electron self-energy shows fine structures associated with the bosonic modes coupled to electrons. In order to precisely determine the energies of the bosons, it is essential to take the second derivative of $Re\Sigma$. Before taking the second derivative of $Re\Sigma$, we need to obtain a smoothed curve for the data. We use a cubic spline interpolation method to smooth the data, which ensures no discontinuity in the first and second derivative. The smoothness of the interpolation is determined by a parameter Λ . The

larger the Λ is, the smoother the curve is. The solid line in Fig. 1a is a smoothed curve with $\Lambda = -2.5$. Fig. 2b shows the $-d^2(Re\Sigma)/d\omega^2$ spectrum obtained from the smoothed curve in Fig. 1a. There are ten peak features at 5.2 meV, 15.2 meV, 26.5 meV, 38.8 meV, 45.0 meV, 60.8 meV, 72.8 meV, 82.8 meV, 89.6 meV, and 96.1 meV. The energies of the peak features match very well with the boson energies (marked by downward arrows) in the electron-boson spectral function obtained using a maximum entropy method [24]. Such an excellent agreement indicates that the smoothed curve in Fig. 1a represents a realistic average of the data.

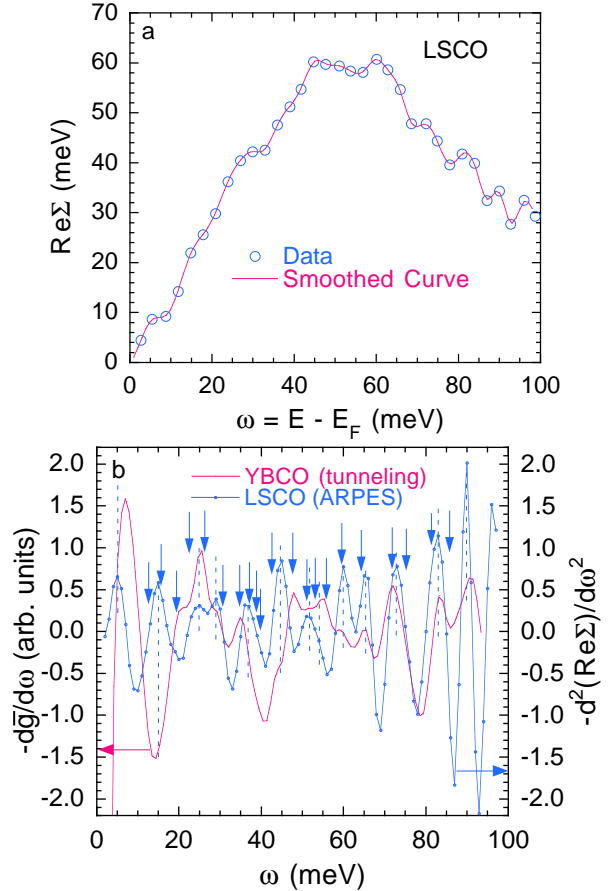


FIG. 2. a) The real part of the electron self-energy at 20 K for the LSCO crystal. The solid line is a smoothed curve obtained using the built-in cubic-spline macro in KleidaGraph. b) The $-d^2(Re\Sigma)/d\omega^2$ spectrum obtained from the smoothed curve in a) and the $-d\bar{g}/d\omega$ tunneling spectrum of $YBa_2Cu_3O_{7-y}$ (Ref. [25]). The downward arrows mark the positions of phonon structures in the high-resolution neutron data of $La_{1.85}Sr_{0.15}CuO_4$ at 20 K below 65 meV and in the lower resolution neutron data at 50 K above 65 meV.

In order to resolve more fine structures in the $-d^2(Re\Sigma)/d\omega^2$ spectrum, one needs to obtain a smooth curve with a smaller Λ . Fig. 2a shows a smoothed curve obtained using the built-in cubic-spline macro in

KleidaGraph. Since the smoothed curve goes through all the data points, this curve should not represent a realistic average of the data, which have an uncertainty of larger than 1 meV. Nevertheless, it is surprising that the positions of the main fine structures in the $-\frac{d^2(\text{Re}\Sigma)}{d\omega^2}$ spectrum of Fig. 2b are the same as those shown in Fig. 1b. In order to check if all the fine structures in $-\frac{d^2(\text{Re}\Sigma)}{d\omega^2}$ are intrinsic, we compare them with the fine structures in the phonon density of states obtained from high-resolution inelastic neutron scattering. The downward arrows mark the positions of phonon structures in the high-resolution neutron data of $\text{La}_{1.85}\text{Sr}_{0.15}\text{CuO}_4$ at 20 K below 65 meV and in the lower resolution neutron data of $\text{La}_{1.85}\text{Sr}_{0.15}\text{CuO}_4$ at 50 K above 65 meV. The phonon peak at 81.3 meV is seen in the lower resolution neutron data of $\text{La}_{1.85}\text{Sr}_{0.15}\text{CuO}_4$ at 50 K but not clearly resolved in the data at 20 K. It is remarkable that the fine structures in $-\frac{d^2(\text{Re}\Sigma)}{d\omega^2}$ match very well with the fine structures in the phonon density of states. Moreover, the fine peak structures in $-\frac{d^2(\text{Re}\Sigma)}{d\omega^2}$ align precisely with the peak/shoulder features in $-\frac{d\bar{g}}{d\omega}$ of $\text{YBa}_2\text{Cu}_3\text{O}_{7-y}$, where \bar{g} is the renormalized tunneling conductance [25]. The peak/shoulder features in $-\frac{d\bar{g}}{d\omega}$ also match precisely with the fine structures in the phonon density of states obtained by inelastic neutron scattering [25]. Therefore, the fine structures in the $-\frac{d^2(\text{Re}\Sigma)}{d\omega^2}$ spectrum of Fig. 2b represent the phonon modes coupled to electrons in $\text{La}_{1.97}\text{Sr}_{0.03}\text{CuO}_4$, which are similar to those in $\text{YBa}_2\text{Cu}_3\text{O}_{7-y}$ due to similar CuO₂ planes.

In Fig. 3a, we show the real part of the electron self-energy at 70 K for a superconducting $\text{Bi}_2\text{Sr}_2\text{CaCu}_2\text{O}_{8+y}$ crystal with $T_c = 91$ K. The data are reproduced from Ref. [26]. The electron self-energy data are obtained from an ARPES spectrum, which is taken with an energy resolution of about 10 meV (Ref. [26]). The fine structures of electron-boson coupling also show up in the electron self-energy of BSCCO. In Fig. 3b, we plot the real part electron self-energy as a function of $\omega = E_F - E - \Delta_D$, where $\Delta_D = 7.0$ meV is chosen to ensure that the first data point is very close to the origin. The solid line is a smooth curve obtained using the built-in cubic-spline macro in KleidaGraph. Taking the second derivative of the smoothed curve yields a $-\frac{d^2(\text{Re}\Sigma)}{d\omega^2}$ spectrum, which is shown in Fig. 3c. We can clearly see that there are 8 peak features at 5.4 meV, 17.0 meV, 25.5 meV, 38.8 meV, 45.2 meV, 60.5 meV, 76.0 meV, and 87.0 meV. The peak features in the $-\frac{d^2(\text{Re}\Sigma)}{d\omega^2}$ spectrum of $\text{Bi}_2\text{Sr}_2\text{CaCu}_2\text{O}_{8+y}$ match very well with those in the $-\frac{d^2(\text{Re}\Sigma)}{d\omega^2}$ spectrum of $\text{La}_{1.97}\text{Sr}_{0.03}\text{CuO}_4$ shown in Fig. 1b. The single peak at 76.0 meV in the spectrum of $\text{Bi}_2\text{Sr}_2\text{CaCu}_2\text{O}_{8+y}$ should correspond to two peaks at 72.8 meV and 82.8 meV in the spectrum of $\text{La}_{1.97}\text{Sr}_{0.03}\text{CuO}_4$. Furthermore, the peak structures in $-\frac{d^2(\text{Re}\Sigma)}{d\omega^2}$ of BSCCO line up precisely with the peak

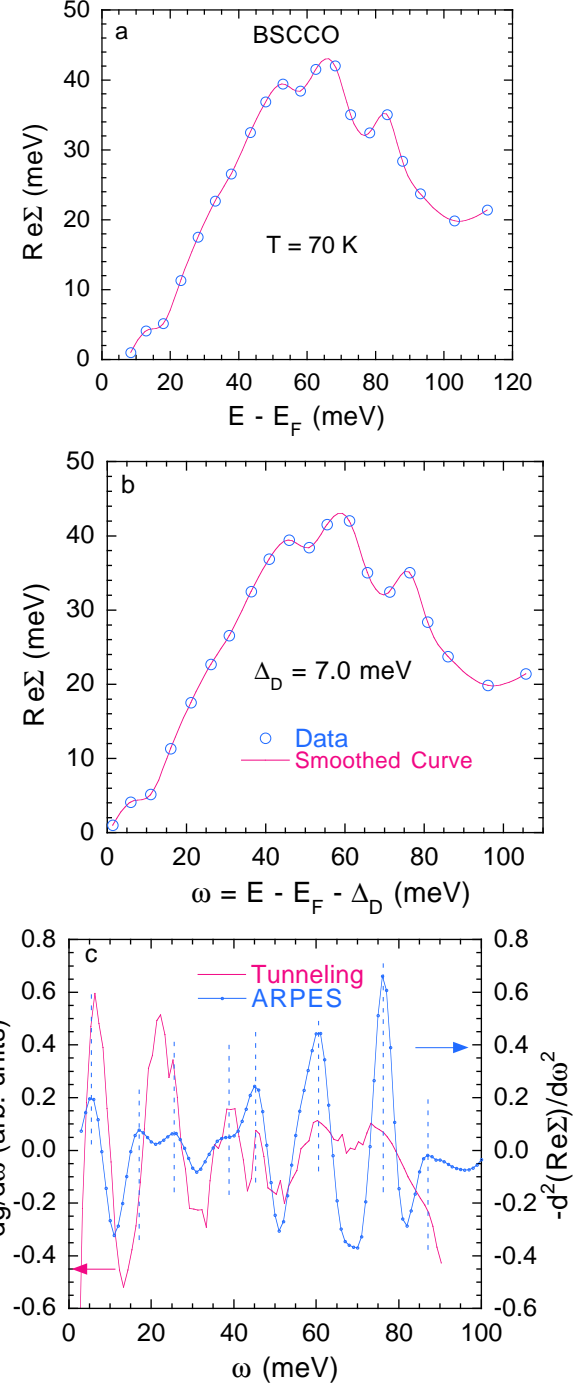


FIG. 3. a) The real part of the electron self-energy at 70 K for a superconducting BSCCO crystal with $T_c = 91$ K. The data are reproduced from Ref. [26]. b) $\text{Re}\Sigma$ versus $\omega = E_F - E - \Delta_D$. Here $\Delta_D = 7.0$ meV is chosen to ensure that the first data point is very close to the origin. The solid line is a smoothed curve obtained using the built-in cubic-spline macro in KleidaGraph. c) The $-\frac{d^2(\text{Re}\Sigma)}{d\omega^2}$ spectrum obtained from the smoothed curve in b) and the $-\frac{d\bar{g}}{d\omega}$ tunneling spectrum of a BSCCO crystal [25].

features in $-\frac{d\bar{g}}{d\omega}$ of BSCCO (Ref. [25]). The peak/shoulder features in $-\frac{d\bar{g}}{d\omega}$ also match precisely

with the fine structures in the phonon density of states obtained by high-resolution inelastic neutron scattering [25]. Such a quantitative agreement among the ARPES, neutron, and tunneling data clearly shows that the fine structures shown in both $-d\bar{g}/d\omega$ and $-d^2(\text{Re}\Sigma)/d\omega^2$ spectra are associated with the phonon modes strongly coupled to electrons.

Since the energies of the phonon fine structures can be precisely determined, the magnitude of the superconducting gap along the diagonal direction can be accurately specified by matching the phonon structures. The value of $\Delta_D = 7.0$ meV at 70 K implies a gap size of about 9 meV at zero temperature from the BCS temperature dependence of the gap. This gap size is comparable with that (12 meV) of the fresh surface of a BSCCO with $T_c = 86$ K (sample #2 of Ref. [11]). As the sample ages, the superconducting gap becomes smaller [11]. This may imply that disorder on the surface can effectively suppress the superconducting gap along the diagonal direction. Furthermore, for a heavily overdoped BSCCO with $T_c = 60$ K the gap along the diagonal direction ($\Gamma - Y$) is also found to be 9 ± 2 meV (Ref. [14]). It appears that the gap along the diagonal direction on the surface of BSCCO is nearly independent of doping in the overdoped region.

In summary, we have analyzed the data of electron self-energy along the diagonal direction of a nonsuperconducting $\text{La}_{1.97}\text{Sr}_{0.03}\text{CuO}_4$ crystal and a superconducting $\text{Bi}_2\text{Sr}_2\text{CaCu}_2\text{O}_{8+y}$ crystal with $T_c = 91$ K. The spectra of the second derivative $-d^2(\text{Re}\Sigma)/d\omega^2$ of the real part of electron self-energy Σ show clear peak features associated with the phonon modes strongly coupled to electrons. For $\text{La}_{1.97}\text{Sr}_{0.03}\text{CuO}_4$ with $\Delta_D = 0$, the energies of the peaks in $-d^2(\text{Re}\Sigma)/d\omega^2$ match precisely with the phonon energies. For $\text{Bi}_2\text{Sr}_2\text{CaCu}_2\text{O}_{8+y}$, the peak energies in $-d^2(\text{Re}\Sigma)/d\omega^2$ also match precisely with the phonon energies obtained from inelastic neutron scattering and single-particle tunneling when Δ_D is set to 7.0 meV. The present results unambiguously demonstrate that the superconducting energy gap along the diagonal direction of $\text{Bi}_2\text{Sr}_2\text{CaCu}_2\text{O}_{8+y}$ is at least 7 meV and that the gap symmetry is not *d*-wave.

*Correspondence should be addressed to
gzhao2@calstatela.edu

Phys. Rev. Lett. **75**, 4516 (1995).

[4] S.-F. Lee, D. C. Morgan, R. J. Ormeno, D. Broun, R. A. Doyle, J. R. Waldrum, and K. Kadowaki, Phys. Rev. Lett. **77**, 735 (1996).

[5] M. Chiao, R. W. Hill, C. Lupien, L. Taillefer, P. Lambert, R. Gagnon, and P. Fournier, Phys. Rev. B **62**, 3554 (2000).

[6] C. C. Tsuei and J. R. Kirtley, Rev. Mod. Phys. **72**, 969 (2000).

[7] A. S. Alexandrov, Physica C **305**, 46 (1998).

[8] J. Betouras and R. Joynt, Physica C **250**, 256 (1995).

[9] J. Mannhart and H. Hilgenkamp, Physica C **317-318**, 383 (1999).

[10] K. A. Müller, Guo-meng Zhao, K. Conder, and H. Keller, J. Phys.: Condens. Matter, **10**, L291 (1998).

[11] Z.-X. Shen et al., Phys. Rev. Lett. **70**, 1553 (1993).

[12] H. Ding et al., Phys. Rev. Lett. **74**, 2784 (1995).

[13] H. Ding et al., Phys. Rev. B **54**, R9678 (1996).

[14] I. Vobornik, R. Gatt, T. Schmauder, B. Frazer, R. J. Kelley, C. Kendziora, M. Grioni, M. Onellion, and G. Margaritondo, Physica C **317-318**, 589 (1999).

[15] G. M. Zhao, Phys. Rev. B **64**, 024503 (2001).

[16] B. H. Brandow, Phys. Rev. B **65**, 054503 (2002).

[17] Q. Li, Y. N. Tsay, M. Suenaga, R. A. Klemm, G. D. Gu, and N. Koshizuka, Phys. Rev. Lett. **83**, 4160 (1999).

[18] A. Bille, R. A. Klemm, and K. Scharnberg, Phys. Rev. B **64**, 174507 (2001).

[19] A. G. Sun, D. A. Gajewski, M. B. Maple, and R. C. Dynes, Phys. Rev. Lett. **72**, 2267 (1994).

[20] I. Maggio-Aprile, Ch. Renner, A. Erb, E. Walker, and O. Fischer, Phys. Rev. Lett. **75**, 2754 (1995).

[21] C. Kendziora, R. J. Kelley, and M. Onellion, Phys. Rev. Lett. **77**, 727 (1996).

[22] A. Bhattacharya, I. Zutic, O. T. Valls, A. M. Goldman, U. Welp, and B. Veal, Phys. Rev. Lett. **82**, 3132 (1999).

[23] G. M. Zhao, Philos. Mag. **84**, 3869 (2004).

[24] X. J. Zhou et al., Phys. Rev. Lett. **95**, 117001 (2005).

[25] G. M. Zhao, cond-mat/0610386.

[26] P. D. Johnson, T. Valla, A.V. Fedorov, Z. Yusof, B. O. Wells, Q. Li, A. R. Moodenbaugh, G. D. Gu, N. Koshizuka, C. Kendziora, Sha Jian, and D. G. Hinks, Phys. Rev. Lett. **87**, 177007 (2001).

[1] J. Bardeen, L. N. Cooper, and J. R. Schrieffer, Phys. Rev. **108**, 1175 (1957).

[2] W. N. Hardy, D. A. Bonn, D. C. Morgan, Ruixing Liang, and K. Zhang, Phys. Rev. Lett. **70**, 3999 (1993).

[3] T. Jacobs, S. Sridhar, Q. Li, G. D. Gu, and N. Koshizuka,